Methodology and comparison of quantitative NO-LIF imaging in a bunsen burner with numerical simulation results

Syed Mashruk[1,*], Richard Marsh[1], Jon Runyon[1], Steven Morris[2], Phil Bowen[1]

1: School of Engineering, Cardiff University, Cardiff, Wales, UK
2: Gas Turbine Research Centre, Cardiff University, Margam, Wales, UK
* Correspondent author: mashruks@cardiff.ac.uk

Keywords: NO LIF, Calibration, Numerical model

ABSTRACT

A planar laser induced fluorescence (PLIF) technique is applied to quantify nitric oxide (NO) concentration in a premixed bunsen burner with a CH_4-air flame doped with NO (up to 1300 ppm). This experimental data will be used as the calibration method for quantitative in-flame NO measurements in a high-pressure generic swirl burner at Cardiff University's Gas Turbine Research Centre. Methodology of modelling premixed bunsen burner combustion experiment in CHEMKIN for predicting NO emissions in a wide variation of premixed methane flames is also described here. Chemical kinetics simulation results from a wide range of fuel flow rates have been compared and analysed with the experimental data in this paper. Our open bunsen burner flame experienced about 15 – 25% reduction in seeded NO level at 25mm above the burner exit. Calibration curves were obtained for both online and offline by measuring NO -PLIF intensity at varying level of NO seeding. These results from both the LIF and simulations will complement each other in subsequent works.

1. Introduction

Increased environmental regulations have made reduced nitric oxide (NO) production an area of intense research across the combustion community. Precise concentration measurement of NO in premixed flames is one of the most crucial part of this investigation as it identifies the location of NO production, which is vital for validating CFD and chemical kinetics models and forlocating areas of above-average NO production. In this pursuit, a LIF technique is applied to measure NO concentration within the flame. The unique excitation properties of laser light allow selective and quantitative probing of many chemical species with high temporal and spatial resolution in combustion environments [1,2]. NO formation mechanisms have already been extensively studied and well documented in literature [3,4] as well as UV LIF of NO, including single point, 1-D line imaging and 2-D planar imaging for understanding NO formation in laboratory flames and practical combustion systems [5-8]. Laser probing for NO measurements have mostly used the A-X system with transitions in the (0,0), (0,1) and the (0,2) bands at 226, 235 and 248 nm respectively

and fluorescence signal detected at 232-252 nm ((0,1)+(0,2) detection), 217-232 nm ((0,0) detection) and 220-240 nm ((0,0)+(0,1) detection) respectively [9-11]. Additionally, some measurements have been taken in the D-X (0,1) band at 193 nm [12] but this band often experiences transmission problems in hot combustion environment. To quantify NO concentrations in the flame from the LIF measurement, the temperature distribution in the flame needs to be accounted for as NO is highly dependent on temperature. This paper aims to describe a qualitative NO measurement process as well as a NO calibration method in an open bunsen burner flame with varying NO seeding level up to 1300 ppm and addresses the difficulties encountered along the way.

2. Experimental Apparatus

Laminar, premixed methane/air flames with lean equivalence ratios (Φ = 0.68 to Φ = 0.87) and rich equivalence ratios (Φ = 1.28 to Φ = 1.4) were stabilized in 15 mm and 25 mm Bunsen burners, respectively, at atmospheric temperature and pressure. NO diluted in nitrogen (1% NO) was blended as a premixed reactant to yield inlet NO concentrations up to 1300 ppm. Constant gas flows were provided by mass-flow controllers (Bronkhorst, three flow controllers for air, methane and NO||N_2, all zero calibrated prior to use). Laser energy density was kept well below 7.5 MW/cm^2 [8] to stay in the linear regime of the NO LIF signal. Fig. 1 depicts the schematic of the NO PLIF experimental setup. The laser induced fluorescence of NO molecule was achieved by tuning the dye laser to 226.03 nm. This wavelength was chosen due to the negligible hot-O_2 interference at atmospheric pressures and maximum signal strength per molecule of NO over a range of temperatures [11]. This excitation wavelength was generated by employing the second harmonic (λ = 532 nm) of a Spectra Physics GCR 170-10 Nd:YAG laser operating at 10 Hz, to pump a Quantel TDL-90-NBP2-UVM3 dye laser. The Nd:YAG laser has a pulse duration of 7-10 ns at 532 nm and resulting linewidth of the TDL-90 dye laser at 560 nm is ±0.005 nm. The pump beam was directed through a series of optical paths in the dye laser, on to the dye cell which was circulated with Pyromethene 597 dye solution. This dye solution has a fundamental frequency of 573 nm when pumped by the 532 nm output from the Nd:YAG laser. Through the use of a diffraction grating (2400 lines/mm), the fundamental frequency was shifted in the dye laser using a remote control with resolution of 0.001 nm. The fundamental frequency (λ_s) was then directed through a frequency-doubling crystal, this frequency doubled beam is then mixed with the residual 1064 nm IR (λ_p) from Nd:YAG laser through a mixing crystal and a Pellin-Broca prism for separation of the desired UV wavelength to excite NO molecules. This mixing after doubling process yields a dye laser output wavelength (λ_{Output}) given in Eq. 1:

$$\lambda_{Output} = \left(\frac{1}{\lambda_p} + \frac{1}{\lambda_s}\right)^{-1} \qquad (1)$$

The Nd:YAG laser produces pulse energies at 532 nm of ~450 mJ/pulse and the dye laser output wavelength of 226.03 nm has a peak energy of ~4 mJ/pulse. The dye laser output beam was then directed through a set of sheet-forming optics to provide a laser sheet approximately 25 mm
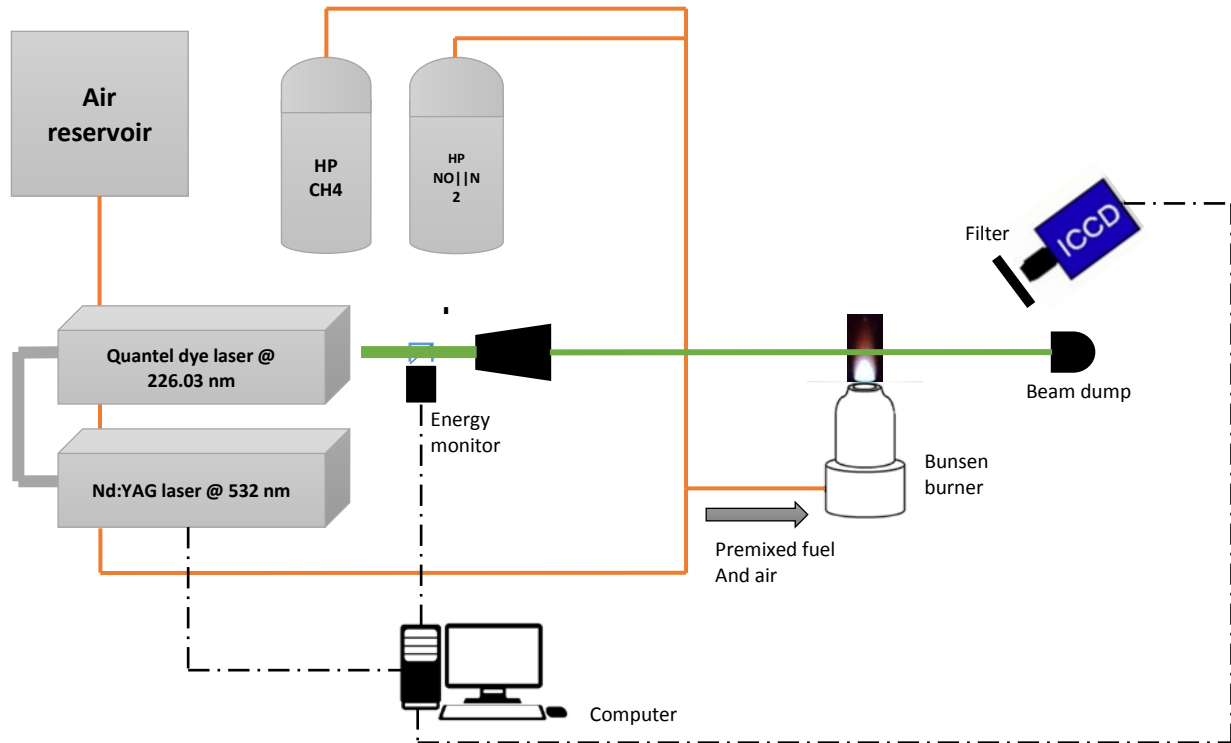

Fig. 1 Schematic of experimental setup for NO LIF measurement.

in width and 2-3 mm thick. The laser sheet was directed along the burner exit nozzle centerline, with varying elevation above the burner exit. For the 25 mm Bunsen burner horizontal orientation, the sheet was horizontal and for the 25 mm burner vertical orientation, the sheet was vertical cutting the flame near the burner exit and for the 15 mm Bunsen burner, the sheet was vertical cutting the flame about 20 mm above the burner exit. A 30R/70T UV plate beamsplitter (Model # 65-922, Edmund Optics) was used to split the laser beam prior to entering the sheet optics and measure respective relative laser energy per pulse to allow for image correction. The resulting fluorescence signal was captured 90° to the laser sheet, through the use of a CCD camera (Dantec HiSense Mk II, 1.3 megapixel resolution) coupled with an image intensifier (Hamamatsu C9546-C03L), 78 mm focal length UV lens (Pentax C91698, f/3.8), and narrow bandpass filters. Image intensifier gate was opened for 100 ns for PLIF measurements and 400 μs for OH chemiluminescence measurements. Image intensifier gain was kept constant at 999 for all PLIF

measurements and at 800 for all chemiluminescence measurements. Two different filter sets were used for qualitative imaging (300 nm shortpass filter, Asahi Spectra Model # ZUS0300 and UG5, Edmund Optics Model # 84-898) and quantitative NO calibration (248 nm bandpass filter with FWHM of 20 nm, Dantec Dynamics and UG5, Edmund Optics). The acquisition period of the ICCD was synchronized with the fluorescence event by providing an appropriate delay with respect to the start of trigger to the Q-switch of the Nd:YAG laser. The fluorescence signal was averaged using 500 laser shots for qualitative and quantitative NO PLIF. The hot O_2 fluorescence interference and background signal were corrected for in the NO fluorescence measurements by tuning the dye laser to an off-line wavelength of 225.94 nm and capturing 200 images. The background signals with the flame were recorded after measuring the NO fluorescence events. True NO PLIF signal was then obtained by subtracting the averaged off-line signal from the averaged on-line signal.

The OH* chemiluminescence system was based on the CCD camera and high-speed gated image intensifier as mentioned above with a OH* filter (315 nm bandpass filter with FWHM of 15 nm, Dantec Dynamics) for wavelength filtering of OH* species chemiluminescence emission. The ICCD was placed at a 90° angle to the direction of flow.

3. Qualitative NO measurement

Qualitative NO PLIF measurements were first made with a 25 mm diameter Bunsen burner placed horizontally in the Gas Turbine Research Centre's High Pressure Optical Chamber (HPOC) [20] as shown in Fig. 2. The flame was asymmetric in this orientation and buoyancy effects were apparent in the flame. However, good evidence of NO production in the flame can be seen in Fig. 3. The laser sheet was traversed along the flame, cutting the flame in the center line of nozzle and NO fluorescence was averaged over 500 shots for this image. As expected, there is limited NO production in the central cold zone, with NO mainly produced in the surrounding hot flame zone due to thermal and prompt NO.

(a)   (b)

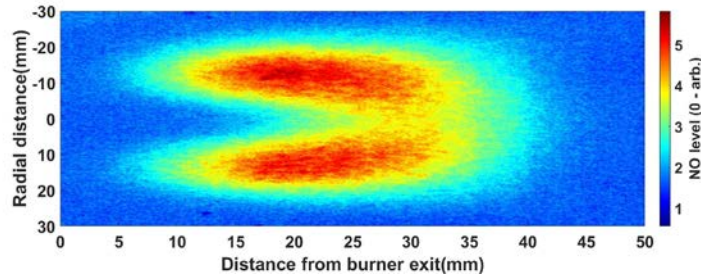Fig. 2 25 mm Bunsen burner horizontal set-up, as installed (a) and with CH_4-air flame (b).

Fig. 3 In-flame NO-LIF signal without NO seeding (ER – 0.88; 2.28 kW). Flow is from left to right.

The burner was then installed vertically outside the HPOC and operated between equivalence ratios of 1.4 and 1.28. This change in equivalence ratio from Φ = 1.4 to Φ = 1.28 was achieved by increasing air flow at constant fuel flow. Thus, as ER is decreased, the flame burning velocity increases and gas velocity decreases. In Fig.4, qualitative NO-LIF measurements from ER 1.4 – 1.28 (a-d) corresponds to the OH* chemiluminescence measurements in Fig. 5 (a-d).
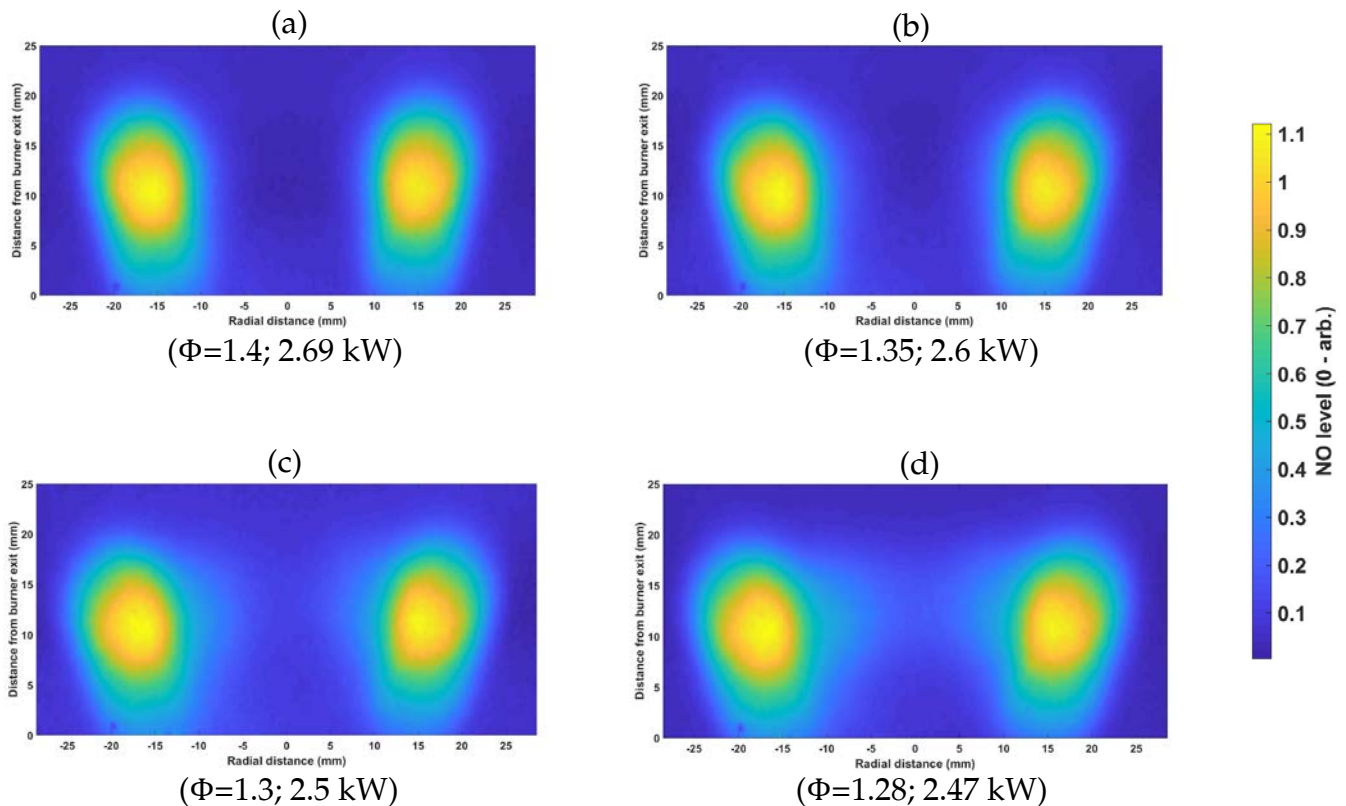

Fig. 4 NO-LIF measurements (a - d) of 25 mm Bunsen burner at varying ER and thermal power. Flow is from bottom to top.

All the images of both Fig. 4 and Fig. 5 are normalized to their respective 1st image (a – EQ 1.4). The flame stabilizes closer to the nozzle and heat release zones are getting stronger between 10 –

20 mm from burner exit as evident by the OH* chemiluminescence in Fig. 5, more thermal and prompt NO is forming within the hot zone as can be seen in Fig. 4. Thus, validating our qualitative NO measurement. However, beyond 20 mm from burner exit, even though the heat release zone is getting stronger, NO is diffused in the atmosphere.
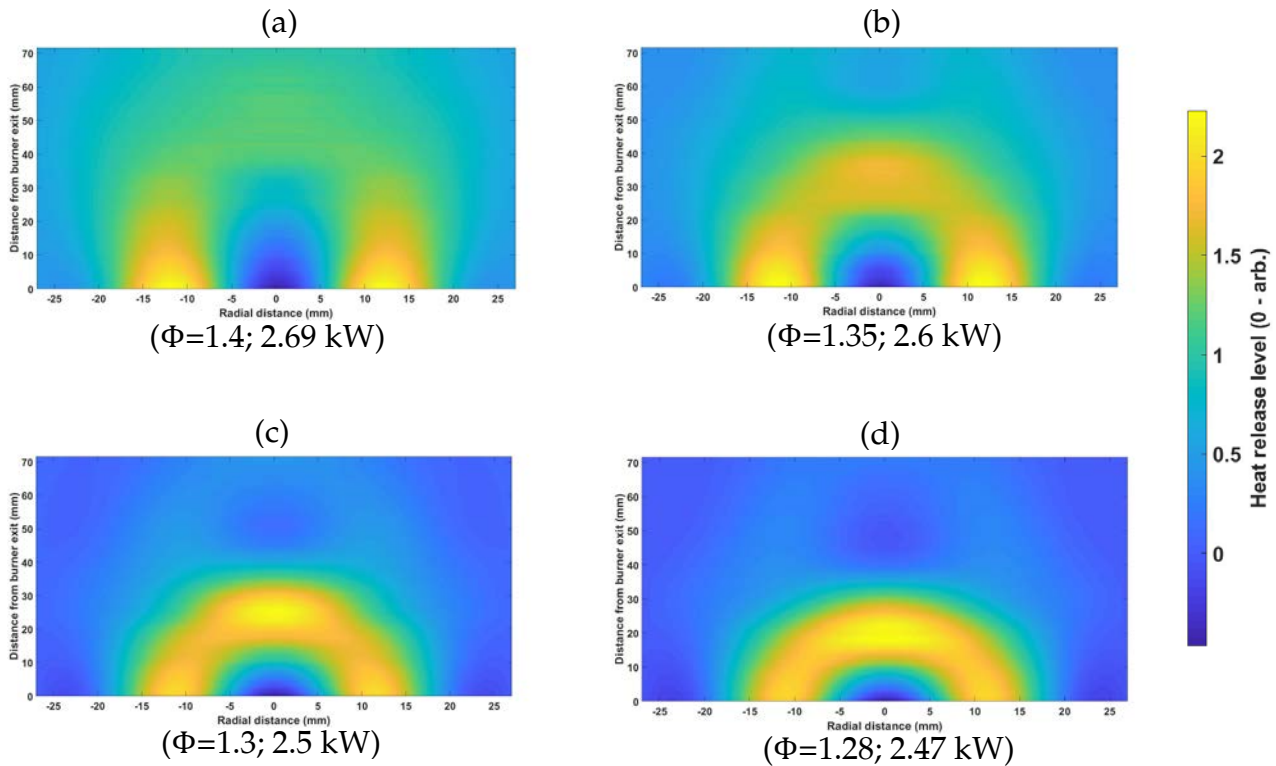

(a)

(Φ=1.4; 2.69 kW)

(b)

(Φ=1.35; 2.6 kW)

(c)

(Φ=1.3; 2.5 kW)

(d)

(Φ=1.28; 2.47 kW)

Fig. 5 OH* chemiluminescence measurement (a - d) at varying ER and thermal power. Flow is from bottom to top.

4. NO Calibration

For two-dimensional LIF diagnostics, calibrating semiquantitative data by using a known concentration of the molecule under study is advantageous as all effects of detection efficiency (e.g. filter transmission) and collisional quenching are accounted for. However, a source of hot NO must be provided for calibration when NO is excited from the second vibrational level [8].

Doping NO in the premixed reactants calibration requires consideration of the interaction between dopant and flame chemistry. Several experiments have investigated the interactions between NO and different flame types [16, 17, 18]. According to Cattolica et al. [17], linear correlation between NO LIF signal and NO concentration remained valid, even after converting 40% NO in flame while doping very high level of NO (4000-8000 ppm) in lean hydrogen/air flames. Reisel and

Laurendeau [18] predicted 5% NO concentration reductions in ethene/air lean flames ($\Phi = 0.9$) in simulation calculations. Flame development and temperatures can also be affected if NO dopant levels are too high Schulz et al. [16] reported that, in a spark-ignition engine fueled with propane/air, only 10% NO was converted in a lean flame ($\Phi = 0.9$) compared to 40% reduction of NO in fuel-rich conditions ($\Phi = 1.25$) at dopant levels of 1000 ppm. In the same experiment no changes in engine performance were found at NO dopant levels of up to 1500 ppm.

Seeded NO(ppm)	CH_4 mass flow (g/s)	Air mass flow(g/s)	Equivalence ratio (Φ)	NO-N_2 mass flow (g/s)	Temperature (K)	NO reading (ppm)	NO lost in flame (%)
1300	0.0079	0.15	0.91	0.0237	1059	1180	9.23%
1000	0.0079	0.15	0.91	0.0177	1062	836	16.4%
800	0.0079	0.15	0.91	0.0138	1067	653	18.4%
700	0.0078	0.15	0.89	0.0120	1033	588	16.0%
600	0.0078	0.15	0.89	0.0101	1051	507	15.5%
500	0.0069	0.15	0.79	0.0083	1013	404	19.2%
400	0.0065	0.15	0.75	0.0065	1025	298	25.5%
300	0.0063	0.16	0.68	0.0051	999	231	23.0%
200	0.0063	0.16	0.68	0.0034	979	166	17.0%
100	0.0063	0.16	0.68	0.0017	1015	81	19.0%
0	0.0063	0.16	0.68	0	1004	11	-

Table. 1 Premixed reactant flow rates, exhaust temperatures, and NO readings for NO dopant level of 0 – 1300 ppm.

For the NO calibration experiment, a 15 mm diameter Bunsen burner was used, and lean methane/air flame was stabilized on the burner nozzle by maintaining approximately equal burning and flow velocities as the NO dopant level changes from 0 – 1300 ppm. Table 1 shows the experimental mass flow rates at different dopant level of NO. Temperature and NO concentration were recorded in the post-flame zone (25 mm above the burner exit) with a K-type thermocouple and a Signal Instruments 4000VM NO_x analyzer. Measurements taken by the NO_x analyzer were hot/wet and not corrected for exhaust oxygen concentration. As seen in Table 1, up to 25.5% of the doped NO was lost in the flame at 400 ppm seeding. With the NO seeding at 1300 ppm, the NO loss in the flame was the lowest observed in the dataset at 9.2%. While some NO loss through the flame was expected, additional losses can be attributed to atmospheric diffusion as the burner

was operated unconfined. The burner was operated leaner as the NO seeding levels were being reduced to stabilize the flame. Fig. 6 illustrates the location of the data point taken at 1300 ppm seeding for the calibration curve in terms of (a) OH* chemiluminescence measurements and (b) NO LIF measurements.
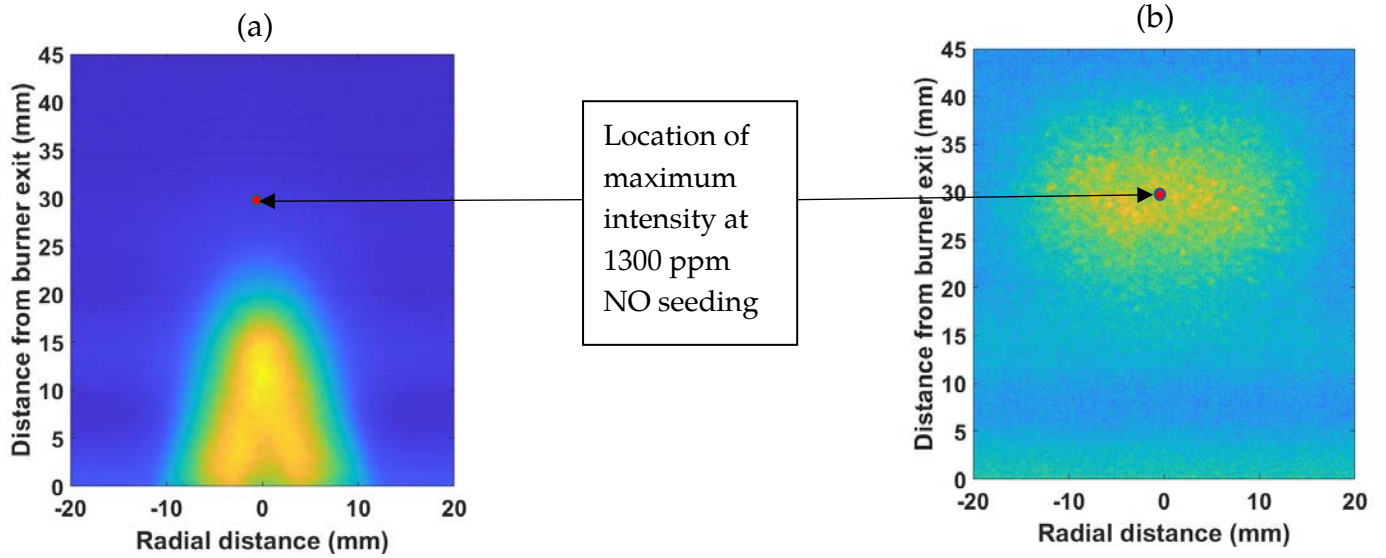

Fig. 6 Location of the data points for the calibration curves in terms of (a) OH* chemiluminescence and (b) NO-LIF measurement.

Thomsen et al. [6] proposed a calibration technique to transfer calibration data from atmospheric conditions to high pressure conditions. This technique assumes that the broadband interferences from O_2, CO_2 and H_2O are relatively constant in value over a range of excitation wavelengths. Fig. 7 represents the calibration curves obtained by varying the amount of NO doped into a reference flame. As both the curves meet at the y axis at 0 ppm seeding, the same background signals (B_c) occurs at both excitation wavelengths. Then, the on-line (S) and off-line (S′) LIF intensities at any point in the doping curve can be written as,

$$S = B_c + S_{NO} \qquad (2)$$
$$S' = B_c + S_{NO}'. \qquad (3)$$

Similarly, the slopes of the two calibration curves m and m′,

$$S_{NO} = m[NO] \qquad (4)$$
$$S_{NO}' = m'[NO] \qquad (5)$$

where [NO] is the total NO concentration, doped plus undoped, in the flame. A factor g can be derived such that,

$$g = \frac{S_{NO}'}{S_{NO}} = \frac{m'}{m}. \qquad (6)$$

From Eq. (2) and (3), the LIF signal for the undoped condition in generic flames can be derived as,

$$S_{NO_u} = S_u - S_u' + S_{NO_u}' \quad (7)$$

where S_u and S_u' are signal of on-line and off-line in undoped condition respectively. Now, using the definition of g,
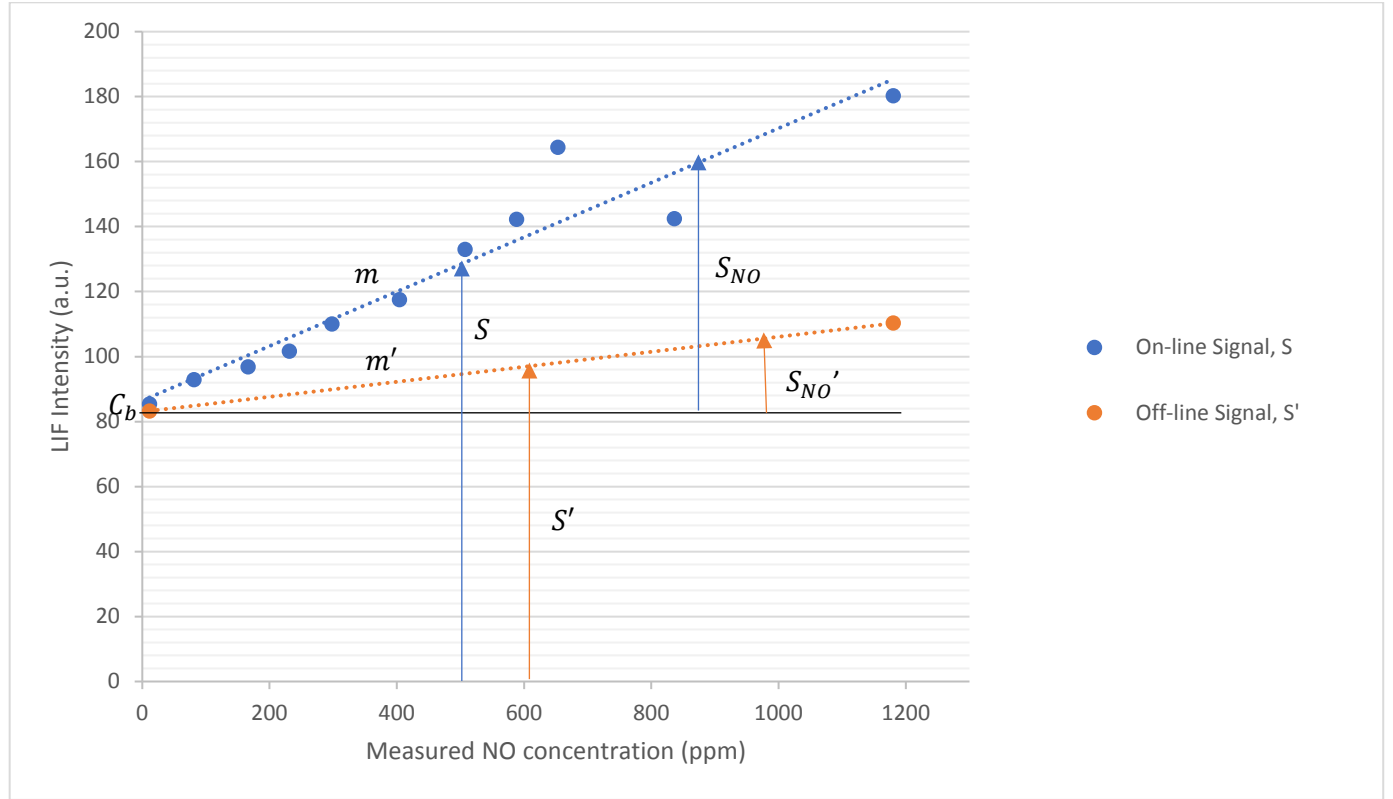
$$S_{NO_u} = S_u - S_u' + gS_{NO_u}. \quad (8)$$

Fig. 7 NO LIF calibration curve for 15 mm Bunsen burner with CH4-air at atmospheric temperature and pressure.

Finally, solving for S_{NO_u} and B_c in terms of g,

$$S_{NO_u} = \frac{(S_u - S_u')}{(1-g)}, \quad (9)$$

$$B_c = \frac{(S_u' - gS_u)}{(1-g)}. \quad (10)$$

According to Ravikrishna et al. [19], the NO concentration in ppm relative to the calibration flame temperature can be expressed as,

$$N_{ppm,RT} = C_b S_{NO_u}. \quad (11)$$

Where C_b is the gradient of the calibration curve. The [NO] in absolute ppm can then be expressed as,

$$N_{ppm,abs} = \left(\frac{T}{T_C}\right)\left(\frac{\gamma_C}{\gamma}\right)\left(\frac{P_C}{P}\right)\left(\frac{I_0}{I_{0,C}}\right)N_{ppm,RT}, \qquad (12)$$

where T is the local flame temperature, P is the local flame pressure, γ is the cumulative correction factor for the effects of collisional quenching, Boltzmann fraction distribution and laser line/absorption line overlap fraction and I_0 is the laser irradiance. The subscript 'C' refers to the quantities in the calibration flame. The cumulative correction factor is obtained using LIFSim tool [13], where temperature, pressure, major species concentrations, excitation wavelengths amongst others are provided as input.

All the raw images are corrected for any non-uniform energy distribution of the laser sheet by using an averaged LIF image of the burner seeded with NO. The images are then corrected for attenuation of the excitation laser light and fluorescence signal, which is dominated by absorption from hot CO_2 with a small contribution from hot H_2O. Attenuation of the laser light and fluorescence signal are corrected on a pixel-by-pixel basis using Beer-Lambert's Law and absorption coefficients known from shock tube measurements [15] and simple consideration of the geometry. These corrections require some knowledge of the local temperature because the CO_2 and H_2O absorption coefficients are temperature dependent and the CO_2 and H_2O number densities are obtained using an assumption of thermal equilibrium in the post-flame gas. Temperature information is also needed to correct for the temperature variation of the NO-LIF signal via the temperature dependence of the laser-excited ground state population, the spectral overlap between the laser-spectral profile and NO absorption spectrum and the fluorescence yield. Thus, NO LIF multi-line thermometry is to be considered in future work for in-flame temperature measurement.

5. Numerical Simulation

The 15 mm Bunsen burner was modelled in CHEMKIN environment as per Fig. 6. Perfectly Stirred Reactors (PSR) were used to model the mixing zone and flame zone and a Plug Flow Reactor (PFR) was used to model the post-flame zone. Two different studies were conducted using GRI-MECH 3.0 [21] mechanism with this model to predict the NO in post-flame zone.

Fig. 8 Simple chemical reactor network model of the 15 mm Bunsen burner in CHEMKIN

In the first study (Fig. 9), the burner was simulated using the maximum heat loss at each condition. As mentioned before, all the NO measurements were taken at 25 mm above the burner exit, however, as NO seeding was reduced from 1300 ppm to 100 ppm, the flame height was reduced as the flame could only be stabilized with the reduced NO flow by reducing the fuel flow. Thus, more heat loss is expected at the reference height as the NO seeding was reduced. Thus, the model predicts lower NO reading at high seeding levels as at these points, the reference height was not sufficient for maximum heat loss to occur. Similarly, as NO seeding concentrations decreased, the model better predicts the measurements.
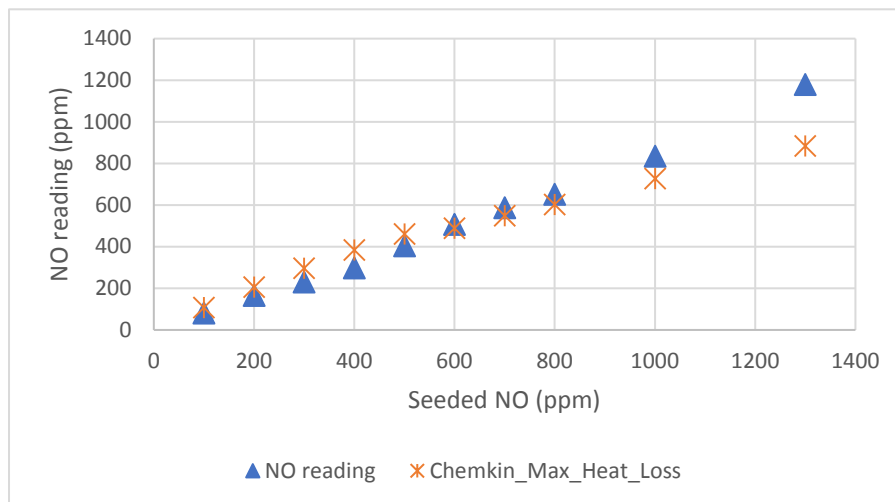

Fig. 9 Comparison of predicted NO with maximum heat loss with actual NO reading.

At 600 ppm, the model predicts the NO reading correctly. However, below 600 ppm, the simulation slightly overpredicts the actual reading. As the flame was getting leaner due to the reduction of fuel with decreased NO seeding, the flame stabilized nearer the burner exit. Thus, the areas of maximum heat release zone were compacted, forming thermal NO in the flame, causing the model to slightly over-predict than the gas analyzer reading.

For the second study (Fig. 10), the modelled heat loss was modified for the 1300 ppm case to match the actual NO reading and the heat loss was then modified as a function of adiabatic flame temperature for the subsequent points. Good agreements were found between the actual and predicted reading in this study.
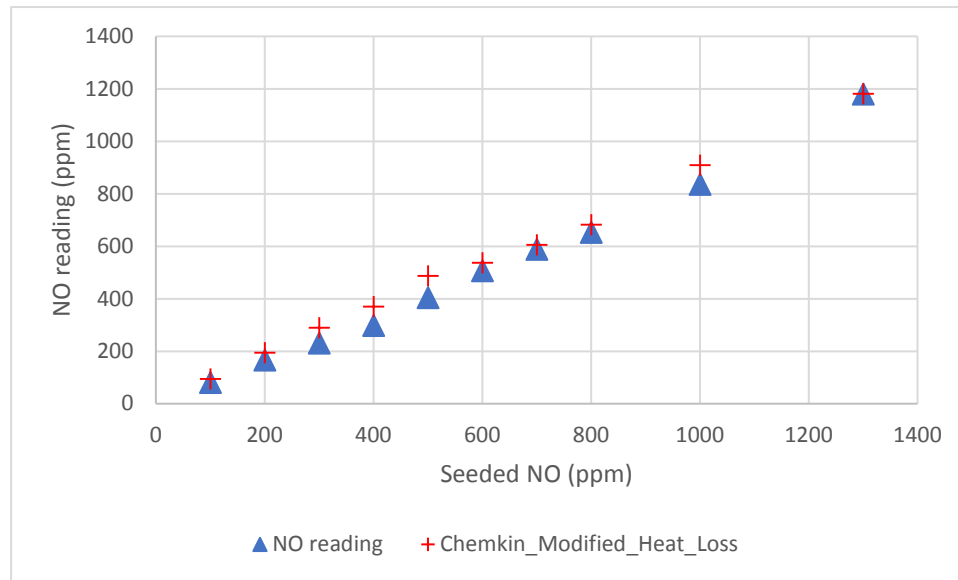
Fig. 10 Comparison of predicted NO with calibrated heat loss with actual NO reading.

6. Conclusions

Qualitative NO PLIF was done with the 25 mm bunsen burner and good relationship was found between increasing heat release level and NO formation. A NO LIF calibration procedure in premixd laminar methane/air Bunsen flames was described in detail in this paper. Linear relationship was found between the maximum intensity value and varrying NO seeding level after applying all the necessery corrections implied. The calibrating technique was implemented to achieve fully quantitative NO concentration values from LIF measurements. Transportability and implementation of the experimental calibration data in a high pressure environment was also mentioned. Care must be taken to be in the linear fluorescence regime while calibrating, otherwise the measurement will not necesserely reflect the actual NO concentraion in the flame as the laser energy will be saturated. Two different numerical simulation studies were compared with the actual NO reading for comparison, with heat loss modelling identified as a key contributing factor in post-flame NO prediction. This study will support future experimentation at the Gas Turbine Research Centre to quantify NO formation in high-pressure swirling flames.

7. Acknowledgements

8. References

[1] Eckbreth AC (1996) Laser diagnostics for combustion temperature and species. Gordon and Breach, Amsterdam.

[2] Wolfrum J (1998) Lasers in combustion: From basic theory to practical devices Symposium (International) on Combustion 27:1-41.

[3] Bowman CT (2000) Pollutants from Combustion, Kluwer Academic Publishers, The Netherlands.

[4] Warnatz J, Maas U, Dibble RW (1997) Combustion, Springer, Berlin-Heidelberg-New York.

[5] Lee T, Jeffries JB, Hanson RK (2007) Experimental evaluation of strategies for quantitative laser-induced-fluorescence imaging of nitric oxide in high-pressure flames (1-60bar). Proc. Combust. Inst. 31:757-764.

[6] Thomsen DD, Kuligowski FF, Laurendeau NM (1997) Background corrections for laser-induced-fluorescence measurements of nitric oxide in lean, high-pressure, premixed methane flames. Applied Optics 36:3244-3252.

[7] Sahu AB, Ravikrishna RV (2016) Quantitative LIF measurements and kinetics assessment of NO formation in H_2/CO syngas-air counterflow diffusion flames. Combustion and Flame 173:208-228.

[8] Schulz C, Sick V, Meier UE, Heinze J, Stricker W (1999) Quantification of NO A-X(0,2) laser-induced-fluorescence: investigation of calibration and collisional influences in high-pressure flames. Applied Optics 38:1434-1443.

[9] Dec JE, Canaan RE (1998) PLIF imaging of NO formation in a DI diesel engine1. SAE Tech. Paper Series 980147.

[10] Jamette P, Desgroux P, Ricordeau V, Deschamps B (2001) Laser induced fluorescence detection of NO in the combustion chamber of an optical GDI engine with A-X(0,1) excitation. SAE Tech. Paper Series 2001-01-1926.

[11] Bessler WG, Schulz C, Lee T, Jeffries JB, Hanson RK (2002) Strategies for laser-induced fluorescence detection of nitric oxide in high-pressure flames. I. A-X excitation. Applied Optics 41:3547-3557.

[12] Andersen P, Meijer G, Schluter H, Voges H, Koch A, Hentschel W, Oppermann W, Rothe W (1990) Fluorescence imaging inside an internal combustion engine using tunable excimer lasers. Applied Optics 29:2392-2404.

[13] Bessler WG, Schulz C, Sick V, Daily JW (2003) A versatile modelling tool for nitric oxide LIF spectra (www.lifsim.com). Proc. Of the Third Joint Meeting of the U.S. Sections of The Comb. Inst. (Chicago, March 16-19, 2003, paper P105).

[14] Feroughi OM, Kronemayer H, Dreier T, Schulz C (2015) Effect of fluctuations on time-averaged multi-line NO-LIF thermometry measurements of the gas-phase temperature. Appl. Phys. B 120:429-440.

[15] Schulz C, Koch JD, Davidson DF, Jeffries JB, Hanson RK (2002) Ultraviolet absorption spectra of shock-heated carbon dioxide and water between 900 and 3050 K. Chem. Phys. Lett. 355:82-88.

[16] Schulz C, Sick V, Wolfrum J, Drewes V, Zahn M, Maly R (1996) Quantitative 2D single-shot imaging of NO concentrations and temperatures in a transparent SI engine. Proceedings of the twenty-sixth international symposium on combustion. 2597-2604.

[17] Cattolica RJ, Cavalowsky JA, Mataga TG (1998) Laser-fluorescence measurements of nitric oxide in low-pressure $H_2/O_2/NO$ flames. Proceedings of the twenty-second international symposium on combustion. 1156-1173.

[18] Reisel JR, Laurendeau NM (1995) Quantitative LIF measurement and modeling of nitric oxide in high-pressure $C_2H_4/O_2/N_2$ flames. Combust. Flame 101:141-152.

[19] Ravikrishna RV, Naik SV, Cooper CS, Laurendeau NM (2004) Quantitative laser-induced fluorescence measurements and modeling of nitric oxide in high-pressure (6-15 atm) counterflow diffusion flames. Combustion Science and Technology 176:1-21.

[20] Runyon J, Marsh R, Bowen P, Pugh D, Giles A, Morris S (2018) Lean methane flame stability in a premixed generic swirl burner: Isothermal flow and atmospheric combustion characterization. Exp Therm Fluid Sci 92: 125-140.

[21] Smith GP, Golden DM, Frenklach M, Moriarty NW, Eiteneer B, Goldenberg M, Bowman CT, Hanson RK, Song S, Gardiner WC, Lissianski VV, Qin Z http://www.me.berkeley.edu/gri_mech/